The Canadian Mineralogist
Vol. 32, pp. 31-41 (1994)

THE CRYSTAL CHEMISTRY OF MANGANESE-BEARING ELBAITE

PETER C. BURNS, DANIEL J. MACDONALD AND FRANK C. HAWTHORNE

Department of Geological Sciences, University of Manitoba, Winnipeg, Manitoba R3T 2N2

ABSTRACT

The structures of eight crystals of manganiferous elbaite, $a \approx 15.90$, $c \approx 7.12$ Å, $V \approx 1560$ Å^3, *R3m*, have been refined to *R* indices of ~2.2% using graphite-monochromated Mo$K\alpha$ X-radiation; the crystals used for the X-ray data collection were analyzed using an electron microprobe. We obtain very close agreement between Li contents estimated from stoichiometric constraints and the results of electron-microprobe analyses, and Li contents calculated from the site-scattering refinements, suggesting that both methods give accurate Li contents for elbaite (where the correct valence state of the transition metals are known). A previously developed relationship between <*Y*–O> and constituent-cation radius shows both Mn and Fe to be completely in the divalent state in these crystals. They all show very strong positional disorder of the *O1* and *O2* anions. This is also a common (although not ubiquitous) feature of many refinements of tourmaline reported in the literature, and may be quantitatively interpreted in terms of local disorder induced by occupancy of the *Y* site by cations of very different size and charge.

Keywords: tourmaline, elbaite, crystal-structure refinement, site populations, chemical compositions.

SOMMAIRE

Nous décrivons les résultats d'affinements de la structure cristalline de huit échantillons d'elbaïte manganifère, ayant, comme paramètres réticulaires *a* et *c*, des valeurs d'environ 15.90 et 7.12 Å, un volume de la maille d'environ 1560 Å^3, et répondant au groupe spatial *R3m*. L'affinement de données obtenues avec rayonnement Mo$K\alpha$ (monochromatisation au graphite) a mené à un résidu *R* d'environ 2.2%. Les cristaux ainsi étudiés ont aussi été analysés par microsonde électronique. Nous obtenons une excellente concordance entre les teneurs en Li prédites selon la stoechiométrie et les résultats d'analyses à la microsonde et celles qui sont indiquées par affinement de la dispersion associée aux sites octaédriques, ce qui fait penser que les deux méthodes sont convenables pour l'elbaïte (dans les cas où la valence des métaux de transition est connue). Une relation établie antérieurement entre <*Y*–O> et rayon cationique montre que Mn et Fe seraient entièrement à l'état bivalent dans ces cristaux. Ceux-ci font preuve d'un désordre de position des anions O1 et O2 très prononcé. Cet aspect, présent dans plusieurs affinements de tourmaline déjà dans la littérature, mais non dans tous, pourrait s'expliquer en termes de désordre local dû à la présence, dans la position *Y*, de cations de dimension et de charge très différentes.

(Traduit par la Rédaction)

Mots-clés: tourmaline, elbaïte, affinement de la structure cristalline, populations des sites, composition chimique.

INTRODUCTION

The determination of the chemical composition of a tourmaline is not a trivial matter. With the electron microprobe, one can analyze for most significant constituents, but not for Li, Fe^{3+}/Fe^{2+} ratio and H, and only recently has it been possible to analyze for B. Traditionally, these components are analyzed by "wet-chemical" methods that involve the dissolution of bulk samples, but such methods are now little used. They require that the material be homogeneous on quite a large scale, a condition that is rarely satisfied in tourmaline. In terms of most components, the advent of electron-microprobe analysis (EMPA) has reduced the analytical problems associated with compositional zoning, but the problems associated with light-element analysis and the valences of transition metals remain.

As part of a general study on the crystal chemistry of tourmaline, here we examine the structural chemistry of manganiferous elbaite. Rossman & Mattson (1986) showed that the unusual yellow and yellow-green colors of these crystals may be due to $Mn^{2+} \rightarrow Ti^{4+}$ charge transfer. These crystals provide an ideal opportunity to test the efficacy of crystal-structure refinement (SREF) for the determination of Li content in tourmaline. In addition, it is of considerable interest to examine the relationship between mean bond-length and constituent-cation radius at the *Y* and *Z* sites in terms of cation order and the possible variations in valence states of the transition metals.

EXPERIMENTAL

Collection of X-ray data

Each of the eight crystals selected for study was ground to (approximate) spheres and mounted on a Nicolet $R\bar{3}m$ automated four-circle diffractometer. Twenty-five reflections were centered using graphite-monochromatized Mo$K\alpha$ X-radiation. The cell dimensions given in Table 1 were derived from the setting angles of the twenty-five automatically aligned reflections by least-squares methods. A total of 1101–1128 symmetry-independent reflections were measured for each crystal ($3 \le 2\theta \le 60°$), with index ranges $0 \le h \le 19$, $0 \le k \le 19$, $-11 \le l \le 11$; reflections forbidden by the R-lattice restriction were not measured. Two standard reflections were measured every 50 reflections; no significant changes in their intensities occurred during data collection. Each data set was corrected for Lorentz, polarization and background effects, and reduced to structure factors. An empirical absorption correction, based on 36 Ψ-scans for each of 11 reflections, was applied to each data set (R-azimuthal given in Table 1).

Refinement of the crystal structure

Scattering curves for neutral atoms, together with anomalous-dispersion corrections, were taken from Cromer & Mann (1968) and Cromer & Liberman (1970), respectively. The Siemens SHELXTL PLUS (PC version) system of programs was used throughout.

Each refinement was done in the space group $R3m$, the space group of all tourmaline species (Grice & Robinson 1989). Starting atomic positional parameters were those of tsilaisite (Nuber & Schmetzer 1984). The final cycles of refinement included anisotropic displacement factors, site-scattering parameters for the X, Y and Z sites, an empirical isotropic extinction correction and a refinable weighting factor g, given by $w = 1/[\sigma^2(F) + \text{abs(g)}F^2]$. Structures were tested for absolute orientation and transformed as appropriate. Final R-indices (Table 1) range from 1.8% to 2.5%, and wR indices from 2.7% to 3.7%. Refined positional parameters and equivalent isotropic displacement factors are given in Table 2, selected interatomic distances in Table 3, and bond angles in Table 4, and refined site-scattering values in Table 5. Anisotropic displacement factors and structure factors may be

TABLE 1. DATA COLLECTION AND REFINEMENT INFORMATION FOR Mn-BEARING TOURMALINE CRYSTALS

	NP1	NP2	NP3	T10	T11	T12	T15	SD
Colour	yellow	light brown	dark brown	yellow-green	yellow-green	brown-green	green	colourless
Locality	Nepal	Nepal	Zambia	Zambia	Zambia	Zambia	Zambia	San Diego Mine
a(Å)	15.932(2)	15.928(1)	15.938(7)	15.872(2)	15.882(7)	15.926(7)	15.802(3)	15.854(2)
c(Å)	7.135(1)	7.137(2)	7.133(5)	7.138(4)	7.123(5)	7.106(4)	7.121(1)	7.106(1)
V(Å^3)	1568.5(4)	1568.1(5)	1569(2)	1557(2)	1556(2)	1561(2)	1539.9(7)	1546.9(4)
Sp. Gp.	R3m	R3m	R3m	R3m	R3m	R3m	R3m	R3m
Z	3	3	3	3	3	3	3	3
Rad/Mon	Mo/Gr	Mo/Gr	Mo/Gr	Mo/Gr	Mo/Gr	Mo/Gr	Mo/Gr	Mo/Gr
<r> (mm)	0.19	0.19	0.10	0.10	0.18	0.16	0.14	0.12
R(az.)	1.38	0.90	0.93	1.23	1.34	1.36	1.47	1.04
R(az.)°	0.81	0.83	0.91	0.95	0.89	0.94	0.93	0.89
#I	1128	1117	1101	1119	1118	1123	1111	1111
# $\lvert F_o \rvert > 5\sigma$	1124	1106	1079	1103	1113	1114	1105	1099
R	2.21	2.31	2.43	2.54	2.33	2.31	2.00	1.82
wR	2.51	3.59	3.34	3.64	3.73	3.32	3.05	2.76
GOF*	1.30	2.69	1.61	1.18	1.40	1.76	1.24	1.05

° denotes corrected for absorption

* GOF = goodness of fit

TABLE 2. FINAL ATOMIC PARAMETERS FOR MANGANIFEROUS TOURMALINE CRYSTALS*+

		NP1	NP2	NP3	T10	T11	T12	T15	SD
X	x	0	0	0	0	0	0	0	0
	y	0	0	0	0	0	0	0	0
	z	0.8408	0.8408	0.8498	0.8408	0.8408	0.8408	0.8408	0.8408
	$U_{eq.}$	191(6)	199(7)	192(9)	238(10)	237(11)	251(9)	215(7)	166(7)
Y	x	0.06188(3)	0.06199(3)	0.06191(3)	0.06188(4)	0.06163(3)	0.06187(3)	0.06178(3)	0.06161(4)
	y	0.93812(3)	0.93801(3)	0.93809(3)	0.93812(4)	0.93837(3)	0.93813(3)	0.93822 (3)	0.93839(4)
	z	0.4431(3)	0.4454(3)	0.4506(4)	0.4477(5)	0.4450(4)	0.4472(4)	0.4472(3)	0.4415(3)
	$U_{eq.}$	123(3)	119(3)	124(3)	126(3)	118(3)	124(3)	114(3)	95(4)
Z	x	0.26101(4)	0.26108(5)	0.26108(5)	0.26101(5)	0.26096(4)	0.26114(5)	0.26043(4)	0.26006(3)
	y	0.29778(4)	0.29784(4)	0.29791(5)	0.29776(5)	0.29770(4)	0.29785(5)	0.29727(4)	0.29682(3)
	z	0.4591(3)	0.4605(3)	0.4674(4)	0.4621(4)	0.4609(4)	0.4617(4)	0.4662(3)	0.4662(3)
	$U_{eq.}$	67(2)	65(2)	68(3)	64(3)	65(2)	67(2)	57(2)	61(2)
Si	x	0.19011(3)	0.19010(4)	0.19012(5)	0.19001(4)	0.18999(4)	0.19001(4)	0.18991(3)	0.18988(3)
	y	0.19206(3)	0.19198(4)	0.19201(4)	0.19194(4)	0.19192(3)	0.19192(4)	0.19188(3)	0.19193(3)
	z	0.0707(3)	0.0724(3)	0.0788(4)	0.0741(4)	0.0723(4)	0.0737(4)	0.0771(3)	0.0758(3)
	$U_{eq.}$	56(2)	53(2)	59(2)	55(2)	53(2)	56(2)	50(2)	50(2)
B	x	0.8904(1)	0.8903(1)	0.8900(1)	0.8904(1)	0.8905(1)	0.8902(1)	0.89068(9)	0.89110(9)
	y	0.1098(1)	0.1097(1)	0.1100(1)	0.1096(1)	0.1095(1)	0.1098(1)	0.10932(9)	0.10890(9)
	z	0.6175(5)	0.6183(5)	0.6252(6)	0.6194(6)	0.6188(6)	0.6198(6)	0.6221(5)	0.6222(4)
	$U_{eq.}$	70(7)	73(8)	77(11)	79(10)	74(8)	76(9)	67(7)	66(7)
O1	x	0	0	0	0	0	0	0	0
	y	0	0	0	0	0	0	0	0
	z	0.2879(7)	0.2888(7)	0.2929(9)	0.2898(8)	0.2894(8)	0.2901(8)	0.2954(6)	0.2955(6)
	$U_{eq.}$	452(17)	450(19)	438(20)	462(21)	444(1)	474(19)	368(13)	263(10)
O2	x	0.93909(8)	0.93898(9)	0.9387(1)	0.9390(1)	0.93882(9)	0.93883(9)	0.93932(7)	0.93980(6)
	y	0.06091(8)	0.06102(9)	0.0613(1)	0.0610(1)	0.06118(9)	0.06117(9)	0.06068(7)	0.06020(6)
	z	0.5909(4)	0.5918(5)	0.5977(6)	0.5933(6)	0.5910(6)	0.5926(6)	0.5914(4)	0.5886(4)
	$U_{eq.}$	216(10)	206(10)	192(11)	204(11)	215(10)	214(10)	171(7)	155(6)
O3	x	0.13447(8)	0.13469(9)	0.1347(1)	0.1345(1)	0.13425(9)	0.13454(9)	0.13356(8)	0.13256(8)
	y	0.86553(8)	0.86531(9)	0.8653(1)	0.8655(1)	0.86575(9)	0.86546(9)	0.86644(8)	0.86744(8)
	z	0.5616(4)	0.5628(4)	0.5693(5)	0.5646(5)	0.5628(5)	0.5644(5)	0.5685(4)	0.5684(4)
	$U_{eq.}$	110(5)	104(6)	111(8)	109(7)	111(6)	109(6)	116(5)	128(5)
O4	x	0.90704(7)	0.90700(8)	0.9068(1)	0.90672(9)	0.90681(8)	0.90671(8)	0.90653(7)	0.90642(7)
	y	0.09296(7)	0.09300(8)	0.0932(1)	0.09328(9)	0.09319(8)	0.09329(8)	0.09347(7)	0.09358(7)
	z	-0.0009(4)	0.0009(4)	0.0080(5)	0.0027(5)	-0.0008(5)	0.0028(5)	0.0047(4)	0.0027(4)
	$U_{eq.}$	92(5)	84(6)	95(7)	87(7)	86(6)	90(6)	84(5)	94(5)
O5	x	0.09309(8)	0.09313(8)	0.0932(1)	0.09340(9)	0.09348(8)	0.09338(8)	0.09344(7)	0.09339(7)
	y	0.90691(8)	0.90687(8)	0.9068(1)	0.90660(9)	0.90652(8)	0.90662(8)	0.90656(7)	0.90661(7)
	z	-0.0235(4)	-0.0213(4)	-0.0141(5)	-0.0197(5)	-0.0211(5)	-0.0195(5)	-0.0180(4)	-0.0200(4)
	$U_{eq.}$	104(5)	95(6)	95(7)	87(6)	99(6)	96(6)	89(5)	99(5)
O6	x	0.1873(1)	0.1874(1)	0.1877(1)	0.1872(1)	0.1872(1)	0.1875(1)	0.18615(9)	0.18490(8)
	y	0.19731(9)	0.1975(1)	0.1976(1)	0.1973(1)	0.1973(1)	0.1974(1)	0.19628(9)	0.19516(8)
	z	0.2954(4)	0.2968(4)	0.3037(5)	0.2982(5)	0.2969(5)	0.2981(5)	0.3015(4)	0.3016(3)
	$U_{eq.}$	88(5)	82(5)	89(6)	86(6)	83(5)	89(5)	80(4)	79(4)
O7	x	0.28611(9)	0.28593(9)	0.2861(1)	0.2859(1)	0.2860(1)	0.2859(1)	0.28598(8)	0.28614(7)
	y	0.28591(9)	0.2858(1)	0.2859(1)	0.2857(1)	0.2858(1)	0.2857(1)	0.28594(8)	0.28646(8)
	z	-0.0101(3)	-0.0086(4)	-0.0016(5)	-0.0069(1)	-0.0081(4)	-0.0071(5)	-0.0029(3)	-0.0030(3)
	$U_{eq.}$	73(4)	67(5)	81(6)	71(6)	71(5)	75(5)	68(4)	66(4)
O8	x	0.2706(1)	0.2706(1)	0.2705(1)	0.2708(1)	0.2708(1)	0.2707(1)	0.27039(9)	0.27000(8)
	y	0.2096(1)	0.2098(1)	0.2098(1)	0.2100(1)	0.2098(1)	0.2100(1)	0.20979(9)	0.20951(9)
	z	0.6293(3)	0.6308(4)	0.6378(5)	0.6320(5)	0.6311(5)	0.6322(5)	0.6365(4)	0.6367(3)
	$U_{eq.}$	88(5)	85(5)	92(6)	88(6)	84(5)	91(5)	78(4)	77(4)

* X, Y and Z site-scattering refined using the scattering factors for Na, Al and Al, respectively.
+ $U_{eq.} = U_{eq.} \times 10^4$.

TABLE 3. SELECTED INTERATOMIC DISTANCES (Å) IN MANGANIFEROUS TOURMALINE CRYSTALS

	NP1	NP2	NP3	T10	T11	T12	T15	SD
X-O2b,f x3	2.450(2)	2.448(3)	2.468(3)	2.437(3)	2.448(3)	2.441(3)	2.432(2)	2.438(2)
-O4b,f x3	2.803(1)	2.808(1)	2.809(2)	2.813(2)	2.804(1)	2.819(1)	2.812(1)	2.815(1)
-O5b,f x3	2.745(1)	2.751(1)	2.749(1)	2.754(1)	2.752(1)	2.761(1)	2.748(1)	2.749(1)
<X-O>	2.666	2.669	2.675	2.668	2.668	2.674	2.664	2.667
Y-O3	2.174(1)	2.174(2)	2.179(2)	2.163(2)	2.166(2)	2.171(2)	2.146(2)	2.147(2)
-O1a	2.036(3)	2.043(3)	2.042(4)	2.040(4)	2.024(4)	2.039(3)	2.007(3)	1.985(2)
-O2b x2	1.996(2)	1.993(3)	1.998(3)	1.984(3)	1.983(3)	1.987(3)	1.966(2)	1.973(2)
-O6c x2	2.034(2)	2.036(2)	2.035(3)	2.034(3)	2.031(3)	2.038(3)	2.000(2)	1.970(2)
<Y-O>	2.045	2.046	2.048	2.040	2.036	2.043	2.014	2.003
Z-O6	1.851(2)	1.850(3)	1.848(3)	1.848(3)	1.846(3)	1.847(3)	1.851(2)	1.861(2)
-O8	1.920(3)	1.918(3)	1.919(3)	1.910(4)	1.913(3)	1.913(3)	1.904(3)	1.905(2)
-O3a	1.971(2)	1.969(2)	1.969(3)	1.965(3)	1.963(2)	1.971(3)	1.955(2)	1.962(2)
-O7d	1.954(2)	1.954(2)	1.953(3)	1.950(3)	1.948(3)	1.951(3)	1.946(2)	1.949(2)
-O7e	1.879(3)	1.880(3)	1.878(4)	1.878(4)	1.876(3)	1.876(3)	1.878(3)	1.882(3)
-O8e	1.886(2)	1.885(2)	1.883(3)	1.880(3)	1.878(3)	1.878(3)	1.878(2)	1.888(2)
<Z-O>	1.910	1.909	1.908	1.905	1.904	1.906	1.902	1.908
Si-O6	1.607(3)	1.606(4)	1.607(5)	1.603(5)	1.603(4)	1.599(4)	1.602(3)	1.609(3)
-O7	1.619(2)	1.617(2)	1.618(2)	1.613(2)	1.613(2)	1.616(2)	1.607(1)	1.613(1)
-O4	1.629(1)	1.627(1)	1.626(2)	1.622(2)	1.621(2)	1.624(2)	1.616(1)	1.623(1)
-O5	1.645(2)	1.643(2)	1.642(3)	1.638(3)	1.636(3)	1.639(3)	1.634(2)	1.639(2)
<Si-O>	1.625	1.623	1.624	1.619	1.618	1.620	1.615	1.621
B-O2	1.357(1)	1.356(1)	1.359(1)	1.348(1)	1.345(1)	1.354(1)	1.349(1)	1.359(1)
-O8a x2	1.383(2)	1.384(2)	1.381(3)	1.383(3)	1.381(2)	1.386(2)	1.379(2)	1.386(2)
<B-O>	1.374	1.375	1.374	1.371	1.369	1.375	1.368	1.377

Equivalent positions: a: y-x, y, z; b: y-x, -x, z; c:x, x-y, z; d: y-x+⅓, -x+⅔, z+⅔; e: -y+⅔, x-y+⅓, z+⅓; f: -y, x-y, z

TABLE 4. SELECTED BOND-ANGLES (°) IN MANGANIFEROUS TOURMALINE CRYSTALS

	NP1	NP2	NP3	T10	T11	T12	T15	SD
O4-Si-O5	103.6(1)	103.7(1)	104.1(1)	104.2(1)	104.3(1)	104.5(1)	104.1(1)	104.1(1)
O4-Si-O7	110.2(1)	110.2(1)	110.2(2)	109.8(2)	104.3(1)	110.1(1)	109.7(1)	109.9(1)
O5-Si-O7	109.5(1)	109.4(1)	109.7(2)	109.1(2)	109.3(2)	109.4(1)	109.0(1)	109.2(1)
O6-Si-O4	112.0(1)	112.1(1)	111.9(2)	112.1(2)	112.1(2)	111.9(1)	111.2(1)	111.8(1)
O6-Si-O5	111.2(1)	111.0(1)	110.9(2)	111.1(2)	111.0(2)	110.9(1)	111.2(1)	110.9(1)
O6-Si-O7	110.2(1)	110.2(1)	109.8(2)	110.3(2)	110.1(1)	110.0(1)	110.6(1)	110.8(1)
O1-Y-O6c x2	97.8(1)	97.6(1)	97.9(1)	97.2(2)	97.8(2)	97.6(1)	98.1(1)	99.9(1)
O2-Y-O2b	93.7(1)	94.0(2)	94.3(2)	94.2(2)	94.6(2)	94.7(1)	94.1(2)	93.1(1)
O3-Y-O2b x2	101.2(1)	101.5(1)	101.2(1)	101.5(2)	101.2(1)	101.6(1)	101.0(1)	100.1(1)
O6-Y-O6c	88.0(1)	87.8(1)	88.2(2)	87.4(2)	87.7(1)	87.8(1)	88.1(1)	89.3(1)
O1-Y-O2b x2	85.6(1)	85.5(1)	85.7(1)	85.8(1)	85.8(1)	85.5(1)	85.0(1)	84.4(1)
O2-Y-O6 x2	89.1(1)	89.0(1)	88.6(1)	89.1(1)	88.8(1)	88.7(1)	88.8(1)	88.7(1)
O3-Y-O6b x2	75.0(1)	75.0(1)	74.8(1)	75.2(1)	74.9(1)	74.9(1)	75.7(1)	75.9(1)
O3-Z-O7e	94.6(1)	94.5(1)	94.7(1)	94.4(2)	94.7(1)	94.6(1)	94.9(1)	95.8(1)
O3-Z-O8e	94.8(1)	94.8(1)	94.8(1)	95.1(1)	94.9(1)	94.8(1)	95.7(1)	96.1(1)
O6-Z-O8	90.8(1)	90.9(1)	90.8(1)	91.2(1)	91.1(1)	90.8(1)	91.4(1)	91.2(1)
O7d-Z-O6	92.5(1)	92.5(1)	92.5(2)	92.4(2)	92.5(1)	92.7(1)	92.5(1)	93.0(1)
O7d-Z-O8	95.9(1)	96.0(1)	96.0(1)	96.0(1)	95.9(1)	95.8(1)	96.1(1)	96.1(1)
O7e-Z-O8e	96.3(1)	96.2(1)	96.2(1)	96.5(1)	96.3(1)	96.0(1)	96.1(1)	95.5(1)
O3-Z-O6	84.2(1)	84.3(1)	84.3(1)	84.4(1)	84.1(1)	84.2(1)	84.0(1)	83.1(1)
O3-Z-O8	92.4(1)	92.4(1)	92.4(1)	92.3(1)	92.4(1)	92.4(1)	91.9(1)	91.6(1)
O6-Z-O8e	94.8(1)	94.8(1)	94.9(2)	94.5(2)	94.7(2)	95.1(1)	94.8(1)	95.4(1)
O7d-Z-O7e	90.1(1)	90.2(1)	90.1(0)	90.3(0)	90.1(0)	90.0(0)	90.0(0)	89.5(0)
O7d-Z-O8e	77.2(1)	77.2(1)	77.2(1)	76.9(1)	77.1(1)	77.2(1)	76.7(1)	76.7(1)
O7e-Z-O8	78.2(1)	78.1(1)	78.1(1)	77.9(1)	78.0(1)	78.2(1)	77.8(1)	77.9(1)
O2b-X-O2b,f x3	72.9(1)	73.1(1)	72.8(1)	73.2(1)	73.1(1)	73.5(1)	72.5(1)	71.9(1)
O2b,f-X-O4b,f x3	70.5(1)	70.6(1)	70.4(1)	70.7(1)	70.6(1)	70.4(1)	71.4(1)	71.4(1)
O2b,f-X-O5b,f x6	86.3(1)	86.5(1)	86.4(1)	86.6(1)	86.4(1)	86.4(1)	87.1(1)	87.0(1)
O4b-X-O4b,f x3	104.9(1)	104.6(1)	105.0(1)	104.3(1)	104.6(1)	104.5(1)	104.1(1)	104.5(1)
O4b,f-X-O5b,f x6	55.2(0)	55.1(0)	55.2(0)	55.0(0)	55.1(0)	55.1(0)	54.9(0)	55.1(0)
O8a-B-O2 x2	121.1(1)	121.0(2)	120.7(2)	121.1(2)	121.2(2)	120.9(1)	121.3(2)	121.5(1)
O8-B-O8a	117.7(2)	118.1(2)	118.7(2)	117.8(2)	117.5(2)	118.2(2)	117.5(2)	117.0(1)

TABLE 5. SITE-SCATTERING (epfu) DERIVED BY SREF AND EMPA VIA STOICHIOMETRIC CONSTRAINTS (M-P), EXPRESSED AS EQUIVALENT ELECTRONS PER SITE

	X site		*Y* site		*Z* site	
	X-ray	M-P	X-ray	M-P	X-ray	M-P
NP1	11.8(1)	11.56	12.9(1)	12.97	12.99(6)	13.0
NP2	11.5(1)	11.42	13.2(1)	13.34	13.00(6)	13.0
NP3	10.8(1)	10.78	15.2(1)	15.06	13.08(6)	13.0
T10	9.1(1)	8.79	8.2(1)	8.73	12.95(8)	13.0
T11	10.4(1)	9.86	12.9(1)	12.66	13.02(6)	13.0
T12	10.1(1)	9.33	13.2(1)	13.03	12.96(6)	13.0
T15	10.2(1)	9.46	13.4(1)	13.29	12.82(5)	13.0
SD	10.2(1)	9.30	10.9(1)	10.66	13.08(5)	13.0
<dev.>	0.47		0.20		0.06	

obtained from the Depository of Unpublished Data, CISTI, National Research Council of Canada, Ottawa, Ontario K1A 0S2.

Chemical analysis

To ensure good chemical constraints for the structure refinements, the single crystals used in the X-ray intensity-data collection were remounted, polished, carbon-coated and analyzed. Electron-microprobe analyses were done on a CAMECA SX–50 instrument in the wavelength-dispersion mode. Beam conditions for all elements were 15 kV, beam current of 20 nA, and a spot diameter of 1 μm. Counting times peak and background determinations for all elements were 20 s and 10 s, respectively. The analytical data were reduced and corrected using the ($\phi\rho z$) method (Pouchou & Pichoir 1984, 1985). The crystals were analyzed with the following standards: albite (Na), orthoclase (K), diopside (Ca, Si), fayalite (Fe), spessartine (Mn), olivine (Mg), chromite (Cr), titanite (Ti), VP_2O_7 (V), kyanite (Al) and fluor-riebeckite (F). The chemical data for each crystal are averages of 10 analyses taken uniformly over each crystal.

The analytical data are summarized in Table 6; structural formulae were calculated on the basis of 31 anions, assuming stoichiometric amounts of H_2O as OH^- (*i.e.*, OH + F = 4 atoms per formula units), B_2O_3 (as BO_3^{3-}), and Li_2O (as Li^+). The amount of Li assigned to the *Y* crystallographic site was taken to be equal to the ideal sum of the *Y* crystallographic sites minus the amount of other cations occupying those sites [Li = 3 – *Y*], and the calculation was iterated to self-consistency. All Mn and Fe was assumed to be divalent; the observed bond-lengths support these assumptions, as do the spectroscopic measurements of Rossman & Mattson (1986).

TABLE 6. RESULTS OF ELECTRON-MICROPROBE ANALYSES* OF MANGANIFEROUS TOURMALINE CRYSTALS

	NP1	NP2	NP3	T10	T11	T12	T15	SD
SiO_2	36.07	36.34	35.68	37.16	36.69	36.90	37.95	37.81
TiO_2	0.39	0.32	0.87	0.26	0.36	0.30	0.04	0.01
Al_2O_3	37.92	37.45	36.09	37.14	37.67	36.89	38.91	41.87
B_2O_3	10.75	10.74	10.59	10.73	10.74	10.69	10.93	11.13
FeO	0.15	1.21	4.71	0.01	0.06	0.33	2.22	0.01
MgO	0.00	0.00	0.02	0.00	0.00	0.00	0.02	0.00
MnO	5.97	5.38	3.52	5.80	5.99	6.23	1.09	0.35
CaO	1.13	0.92	0.83	0.32	0.31	0.25	0.45	1.02
Na_2O	2.15	2.32	2.17	2.46	2.37	2.45	2.26	1.61
K_2O	0.03	0.03	0.04	0.03	0.03	0.03	0.02	0.01
Li_2O	1.62	1.58	1.38	1.58	1.52	1.53	1.90	2.13
H_2O	3.10	3.11	3.14	3.10	3.19	3.06	3.14	3.34
F	1.29	1.25	1.08	1.27	1.09	1.33	1.33	1.05
O=F	-0.54	-0.53	-0.45	-0.53	-0.46	-0.56	-0.56	-0.44
Total	100.03	100.13	99.66	99.90	99.32	99.56	99.43	99.70
Si	5.83	5.88	5.86	6.00	5.94	5.99	6.00	5.90
Al	0.17	0.12	0.14	0.00	0.06	0.01	0.00	0.10
ΣSi	6.00	6.00	6.00	6.00	6.00	6.00	6.00	6.00
Al	6.00	6.00	6.00	6.00	6.00	6.00	6.00	6.00
ΣZ	6.00	6.00	6.00	6.00	6.00	6.00	6,00	6.00
Ti	0.04	0.04	0.11	0.03	0.04	0.04	0.01	0.00
Al	1.07	1.01	0.84	1.11	1.14	1.05	1.32	1.61
Fe	0.02	0.16	0.65	0.00	0.01	0.05	0.29	0.00
Mg	0.00	0.00	0.01	0.00	0.00	0.00	0.01	0.00
Mn	0.82	0.74	0.49	0.80	0.82	0.86	0.15	0.05
Li	1.05	1.03	0.90	1.04	0.99	1.00	1.22	1.34
ΣY	3.00	3.00	3.00	3.00	3.00	3.00	3.00	3.00
Ca	0.20	0.16	0.15	0.06	0.05	0.04	0.08	0.17
Na	0.67	0.73	0.69	0.77	0.74	0.77	0.70	0.49
K	0.01	0.01	0.01	0.01	0.01	0.01	0.00	0.00
ΣX	0.88	0.90	0.85	0.84	0.80	0.82	0.78	0.66
OH	3.34	3.36	3.44	3.35	3.44	3.32	3.33	3.48
F	0.66	0.64	0.56	0.65	0.56	0.68	0.67	0.52
ΣOH	4.00	4.00	4.00	4.00	4.00	4.00	4.00	4.00

* Li_2O, B_2O_3, H_2O estimated by stoichiometry. Results of analyses reported in wt%.

Discussion

Compositional determination by SREF and EMPA.

SREF is an electron-counting technique with spatial resolution, and can, in principle, solve well-constrained analytical problems (Hawthorne & Grice 1990). Although the size of the crystal required for SREF is significantly larger (100–200 μm) than the diameter of an electron (microprobe) beam, it still provides a "milli-probe" determination of the additional components. Indeed, EMPA of the actual crystal used to collect the X-ray intensity data provides extremely good control of chemical variation.

B site: It is possible to determine the concentration of B by EMPA, but at the present time, this is at the limits of the instrument, and results are relatively imprecise. Thus, even if the B determination is accurate, considerable error can be introduced into a calculation of the formula-unit of tourmaline *via* the imprecision of the analyzed B content. On the other hand, SREF is

quite sensitive to the presence of B, particularly if it is in solid solution with another (possibly much heavier) scattering species. In the present case, the *B* position is assigned as being fully occupied by B, and the observed equivalent isotropic displacement factors are compatible with this assignment. There is no sign of significant vacancies at the *B* site. Small amounts of substitution of B by C or N would not greatly perturb the scattering relationships, but would considerably reduce the observed <*B*–O> bond length below the value typical for [3]-coordinated B. As is apparent from Table 3, this is not the case. The observed <*B*–O> distance of 1.373 Å is comparable with $<^{[3]}$B–O> distances in a wide range of mineral and inorganic structures. Thus the structure results are compatible with full occupancy of the *B* site by B. Any B in excess of 3 apfu would be easily visible, either by observed density at a new site or by a reduction of scattering at the *Si* site (occupation of the *Y* site is not feasible as $^{[6]}$B has never been observed in an oxide environment). Neither of these situations is observed, and thus we may conclude that B is present in these crystals in a fixed stoichiometric amount; unit formulae (Table 6) were calculated on this basis.

Z site: The *Z* site-scattering refined to values compatible with occupancy by Al and Mg. It has been shown that Mg can occur at this site (Hawthorne *et al.* 1993), but this cannot be the case for these crystals, as EMPA data show them to have no significant Mg (Table 6).

Y site: In the present case, the problem is particularly straightforward as the tourmaline samples examined here are essentially Fe-free, and hence there is no Fe^{3+}/Fe^{2+} problem. Furthermore, the spectroscopic results of Rossman & Mattson (1986) on the same crystals showed Mn to be present only in the divalent state. Consequently, the main problem here concerns the determination of Li content. From a chemical point of view, this problem must be dealt with during the calculation of the formula unit from the electron-microprobe data, as the details of the calculation are significantly affected by the Li content. Here, we assumed that Li occupies only the *Y* site and estimated the Li content by difference, iterating the calculation to self-consistency. The resulting cations assigned to the *Y* site (Table 6) can then be used to calculate the effective X-ray scattering at this site in each crystal. The X-ray scattering at this site is actually measured by site-scattering refinement during the SREF procedure. These values are given in Table 5. The agreement between the effective scattering at each site from the two methods is extremely close, with a mean absolute deviation of 0.20 e/site, confirming the estimates of the Li content. The measure of agreement between the two sets of data can also be expressed in terms of composition: when distinguishing between Li (Z = 3) and Al (Z = 13), both typically occur in the *Y* site, and 0.20 e corresponds to a difference of 0.02 Li atoms per site. Thus the agreement between the two methods indicates a high level of accuracy in the determination of Li by these two methods in the case of the elbaite crystals examined here.

X site: The electron-microprobe data show this site to contain significant Na and Ca, with trace K and significant vacancies present. A comparison of the SREF and EMPA results is given in Table 5. The discrepancy between the two sets of results is somewhat greater for this site than for the *Y* and *Z* sites. It is small for crystals TNP1 to TNP3 and TSD, in which the equivalent isotropic displacement factor is less than 0.02, but larger for crystals T10 to T15, in which the isotropic displacement factor is greater than 0.02. For crystals T10 to T15, fixing the isotropic displacement factor at 0.019 leads to good agreement between the refined scattering at the *X* site and the site population as assigned from the electron-microprobe data. This argument suggests that the anisotropic displacement model for crystals T10 to T15 is not quite adequate. However, the discrepancies are still significantly less than 1.0 e per formula unit for these crystals.

Positional disorder of anions in tourmaline

A conspicuous characteristic of the anion parameters in Table 2 is the wide range of values of the equivalent isotropic displacement factors for the anion positions. They vary *within* each structure by a factor of 5 or so, but are very consistent across the range of structures examined. The maximum values are for the *O*1 position with a U_{eq} of approximately 0.045, next are the values for *O*2 that cluster around a U_{eq} of 0.021, and for *O*3, a U_{eq} of 0.011; values for the other anion position are all less than 0.010. This pattern of behavior is common to many of the refined structures of tourmaline described in the literature [buergerite (Barton 1969), liddicoatite (Nuber & Schmetzer 1981), schorl (Fortier & Donnay 1975), tsilaisite (Nuber & Schmetzer 1984), and alkali-deficient schorl (Foit 1989)], although some show it to a lesser degree [feruvite (Grice & Robinson 1989)], and in other types it is absent [dravite (Schmetzer *et al.* 1979, Hawthorne *et al.* 1993), uvite (Schmetzer *et al.* 1979), and V-bearing tourmaline (Foit & Rosenberg 1979)]. This is evidently a significant feature of the tourmaline structure and is worthy of further consideration.

In the following discussions, all of the difference-Fourier maps were calculated while omitting the scattering species from the specific site of interest (in this way, errors due to series termination are minimized). Figure 1 shows the *O*1 site for tourmaline TNP2; (a) is a (001) section, and (b) is a (100) section. The delocalization of density in the (001) plane is very

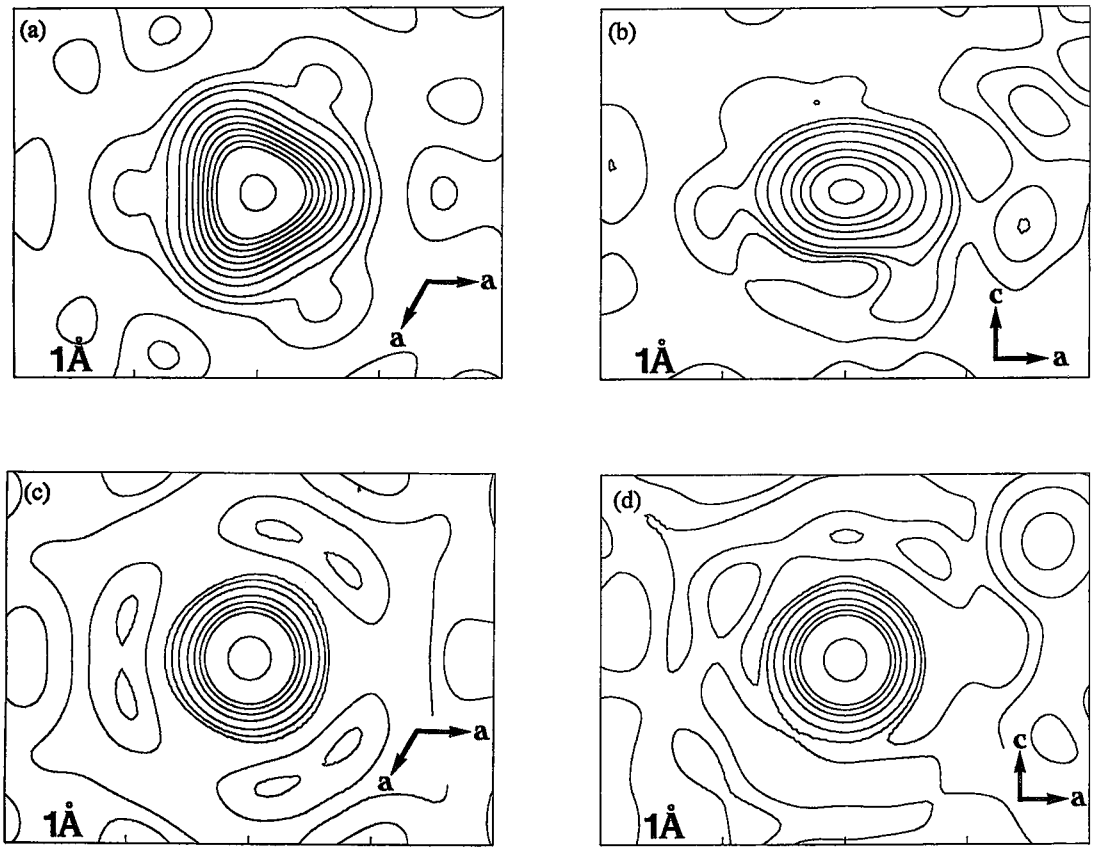

FIG. 1. Difference-Fourier maps around the *O1* site in manganiferous elbaite TNP2 (a,b) and dravite (c,d): (a) (001) section; (b) (100) section; (c) (001) section; (d) (100) section. Contour interval = 2 e/Å^3; note the significantly greater delocalization of electron density (disorder) in the manganiferous elbaite as compared with the dravite.

noticeable in the (100) section (Fig. 1b), and the (001) section shows that this delocalization has a 3-lobed character, with preferential delocalization along the three principal axes in the (001) plane. This contrasts with the behavior of the same site in dravite (Figs. 1c,d), which shows a much more isotropic distribution of density, although there is still some sign of slight delocalization along the *x*, *y* and *u* axes in dravite (Fig. 1c). Figure 2 shows similar maps for the *O2* site. In tourmaline TNP2, the (001) section shows significant anisotropy in the (001) plane, with elongation in two directions, but the (100) section shows no sign of any delocalization along [001]. In contrast, the same site in dravite (Figs. 2c, d) shows much more isotropic behavior, although there is still some indication of slight anisotropy in Figure 2c.

It seems a reasonable supposition that the large anisotropic displacements of *O1* and *O2* in some varieties of tourmaline are due primarily to positional disorder rather than to thermal vibration, as general geometry of bonds controls the vibrational behavior and is essentially unchanged from one tourmaline mineral to another. This line of argument is also suggested by the fact that the displacement factors for the *Y* cations parallel the variation of the displacement factors at *O1* and *O2*, albeit at much reduced values. We attempted to model these displacements during the refinement procedure in the following manner: (1) the *O1* atom was displaced off the 3-fold axis (position 3*a*) in the mirror plane (position 9*b*); (2) the *O2* atom was split into two half-occupied sites; displacement factors for *O1* and *O2* were considered isotropic and fixed at the average isotropic displacement value for the other anion positions in the structure. Full-matrix least-squares refinement converged to significantly lower *R*-indices (Table 7) than before (Table 1), giving what we contend is a more realistic physical model. Except for the *O1* and *O2* sites, the result of these refinements were not found to be noticeably different from those of Table 2; the parameters for the displaced *O1* and *O2* sites are given in Table 7.

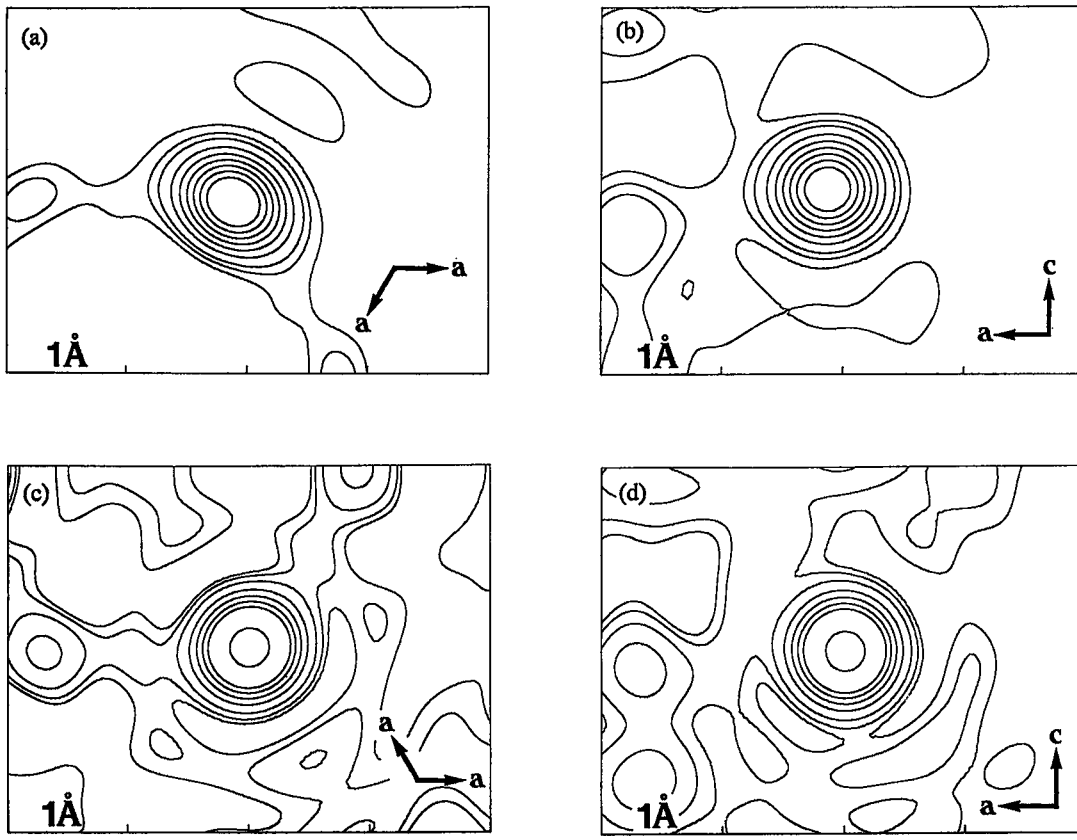

FIG. 2. Difference-Fourier maps around the *02* site in manganiferous elbaite (a,b) and dravite (c,d); (a) (100) section; (b) (001) section; (c) (100) section; (d) (001) section; legend as in Figure 1.

TABLE 7. SPLIT-SITE REFINEMENT RESULTS (DISTANCES IN Å) FOR MANGANIFEROUS TOURMALINE CRYSTALS

	NP1	NP2	NP3	T10	T11	T12	T15	SD
R (%)	2.02	2.03	2.32	2.33	2.13	2.15	1.88	1.84
01 x	0.0119(2)	0.0111(2)	0.0107(2)	0.0112(2)	0.0109(2)	0.0113(2)	0.0097(1)	0.0077(2)
02 x	0.9287(2)	0.9490(2)	0.9481(3)	0.9488(2)	0.9490(2)	0.9490(2)	0.9477(2)	0.9474(2)
y	0.0507(2)	0.0712(2)	0.0707(3)	0.0711(2)	0.0715(2)	0.0715(2)	0.0693(2)	0.0681(2)
Y-01a	1.790(3)	1.794(3)	1.804(4)	1.794(4)	1.783(4)	1.788(4)	1.788(3)	1.802(3)
Y-01a' x2	2.178(4)	2.187(5)	2.180(2)	2.188(5)	2.167(5)	2.189(5)	2.133(4)	2.079(4)
Y-02b x2	1.877(3)	1.876(3)	1.889(4)	1.869(4)	1.866(3)	1.868(3)	1.869(3)	1.884(3)
Y-02b' x2	2.119(3)	2.115(4)	2.111(4)	2.104(4)	2.106(3)	2.111(3)	2.068(3)	2.066(3)
Y-03	2.176(1)	2.175(2)	2.182(2)	2.165(2)	2.168(2)	2.173(2)	2.147(1)	2.150(2)
Y-06 x2	2.033(2)	2.035(2)	2.036(3)	2.034(3)	2.030(2)	2.038(3)	1.999(2)	1.969(2)
B-02	1.360(4)	1.361(4)	1.364(5)	1.353(5)	1.350(4)	1.359(4)	1.353(4)	1.363(4)
-08a x2	1.385(2)	1.385(2)	1.382(3)	1.384(2)	1.383(2)	1.387(2)	1.379(2)	1.384(2)

Mean bond-lengths in tourmaline

Hawthorne *et al.* (1993) attempted to derive relations between mean bond-length and constituent-cation radius for the *Y* and *Z* sites in the tourmaline structure. However, they regarded their relationships as preliminary, partly owing to the paucity of data, and partly owing to a lack of knowledge of the valence state of Fe in some refined structures of tourmaline. Once established for chemically simple and well-characterized structures, such relationships are extremely useful in deriving the oxidation state of transition metals and cation-ordering patterns in the more complex chemical variants.

The Z site: The *Z* sites are occupied essentially by Al. Site-scattering refinement suggests that there may be slight amounts of Fe present in some cases, up to 0.015 atoms per site, but this will have a negligible effect on the observed mean bond-lengths (*i.e.*, a total spread of 0.002 Å). Thus the small amount of scatter (±0.004 Å) in the <Z–O> values is presumably due to inductive effects rather than compositional variation. This is in agreement with the curve for the *Z* site produced by Hawthorne *et al.* (1993).

The Y site: Figure 3 shows the curve for the *Y* site (Hawthorne *et al.* 1993), together with the results of the present work. First, four of the crystals, NP1, T10, T11 and SD, have negligible (≤0.02 apfu) Fe, and hence the valence state of Fe is not a factor (*i.e.*, problem) in calculating the mean constituent-cation radius. Mn could potentially be divalent or trivalent, but the data fall close to the proposed line for Mn^{2+} only, in agreement with the usual assignment of valence for Mn as indicated by stoichiometry and spectroscopic measurements (Nuber & Schmetzer 1984, Schmetzer & Bank 1984, Rossman & Mattson 1986, Shigley *et al.* 1986). For the crystals with significant (≥0.05 apfu) Fe, the data show uniformly good agreement with the proposed line if all of the Mn and Fe is divalent. The horizontal lines in Figure 3 show the possible variations in constituent-cation radius with all Mn divalent and Fe ranging from trivalent to divalent; these variations indicate that there is negligible Fe in the trivalent state in these specimens of tourmaline. Thus Figure 3 shows that both Mn and Fe are completely divalent in these crystals, and establishes that the curve shown is a reasonably good working relationship between mean bond-length and constituent-cation radius in tourmaline. When more data become available, particularly on tourmaline crystals with very different anion contents, it will be worthwhile to include the effects of anion variations at *O1* and *O3*.

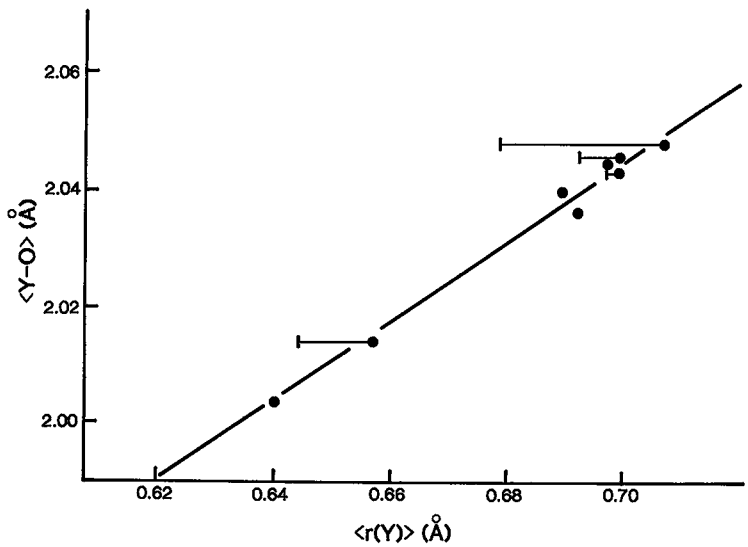

FIG. 3. Relationship between <*Y*–O> and constituent *Y*-cation radius (curve from Hawthorne *et al.* 1993). Horizontal lines show the variation in constituent-cation radius as a function of the Fe^{3+}/Fe^{2+} ratio; symbols with no associated horizontal lines are Fe-free. Note that the curve is compatible with all Fe in the divalent state.

Positional disorder at 01 and 02

The split-site refinements for the *01* and *02* anions produced significant displacements from the ideal positions, with *01–01* and *02–02* "separations" of ~0.5 and ~0.3 Å, respectively, for all crystals. It is notable that only the *Y*–O distances are significantly affected by these displacements, suggesting that the displacements are associated with different local-occupancy configurations at the trimer of *Y* sites in the structure. The resulting *Y*–O distances are given in Table 7, and a diagram of the local displacements and the neighboring positions is given in Figure 4. The *Y*–O distances given in Table 7 are all the possible single separations, and it is necessary to select from these the combinations of distances that are possible as discrete configurations of the coordination. This may be done *via* inspection of Figure 4. For example, *01* is displaced toward one of the three surrounding *Y*-sites; thus one site has one short *Y–01* distance, and the other two sites have long *Y–01* distances. Similarly, *02* is displaced off the mirror plane toward one of the two neighboring *Y* cations; thus there is one long *Y–02* distance and one short *Y–02* distance.

There are six possible local arrangements with <*Y*–O> distances of 1.96, 2.00 and 2.04 Å (for *Y–01*a ≈ 1.79 Å) and 2.03, 2.07 and 2.11 Å (for *Y–01*a′ ≈ 2.18 Å). Examination of the unit formulae of these crystals (Table 6) shows that there are three principal *Y* cations: Al, Li and Mn^{2+}, the expected octahedral sizes for which correspond best to the local arrangements with <*Y*–O> distances of 1.96, 2.07 and 2.11 Å, respectively. These three arrangements fit together very well (Fig. 5). The Al site requires a short *Y–01*a distance, whereas the Li and Mn sites require long *Y–01*a distances. The Mn site requires two long *Y–02*b distances, which force short *02*b–Li and *02*b–Al distances. The Li site requires one short and one long Li–*02*b distances, which forces the second Al–*02*b distance to be short (Fig. 5). The configuration shown in Figure 5 fits together very well, suggesting that it may be a locally ordered trimer that could account for the tendency of these tourmaline crystals to have a *Y*-site composition of approximately $[Li_1(Mn^{2+}+Fe^{2+})_1Al_1]$. Of course, this ordered trimer would show orientational disorder to conform with long-range rhombohedral symmetry.

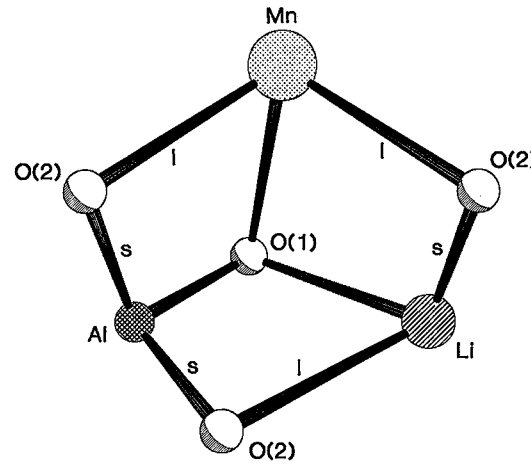

FIG. 5. Proposed dominant local arrangement in manganiferous elbaite; the letters "l" and "s" denote long and short bonds, respectively, relative to the bonds to *01* and *02* at their ideal positions.

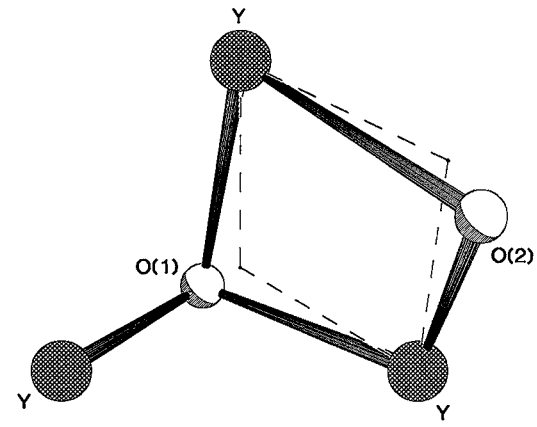

FIG. 4. A sketch of a set of coupled displacements associated with local disorder at the *01* and *02* sites. The broken lines show the bonds from the *Y* cations to the ideal positions of the *01* and *02* anions. The displacements of the *01* and *02* anions from their ideal positions are exaggerated for clarity.

CONCLUSIONS

(1) We obtain very close agreement between Li contents estimated from stoichiometry constraints in the renormalization of the electron-microprobe data, and Li calculated from site-scattering refinement, suggesting that both methods give accurate Li contents for elbaite (where the valence states of the transition metals are known).

(2) Consideration of mean bond-lengths shows that both Mn and Fe are completely in the divalent state in the elbaite crystals examined here, in agreement with previous results on stoichiometry and spectroscopy (Mattson & Rossman 1984).

(3) The relationship between <*Z*–O> and <*Y*–O> and constituent-cation radii produced by Hawthorne *et al.* (1993) agrees well with the structural results given here.

(4) Some varieties of tourmaline show very prominent positional disorder at the *01* and *02* anion positions, and the character of this disorder is very consistent from structure to structure. This disorder may be quantitatively interpreted in terms of local disorder at the edge-sharing trimer of *Y* octahedra, associated with occupancy of the *Y* sites by cations of very different charge and radius (Li, Mn^{2+} and Al in the case of the crystals of manganiferous elbaite examined here).

Acknowledgements

We thank George R. Rossman (California Institute of Technology) for contributing the material used in this work. Financial support was provided by the Natural Sciences and Engineering Research Council of Canada in the form of Post-graduate Fellowships to PCB and DJM, and Operating, Equipment and Infrastructure Grants to FCH. The quality of this contribution was improved after reviews by Dr. Karl Schmetzer and an anonymous reviewer, and editorial work by Drs. Robert F. Martin, Ronald C. Peterson, and Robert T. Downs.

References

Barton, R., Jr. (1969): Refinement of the crystal structure of buergerite and the absolute orientation of tourmalines. *Acta Crystallogr.* **B25**, 1524-1533.

Cromer, D.T. & Liberman, D. (1970): Relativistic calculation of anomalous scattering factors for X rays. *J. Chem. Phys.* **53**, 1891-1898.

——— & Mann, J.B. (1968): X-ray scattering factors computed from numerical Hartree–Fock wave functions. *Acta Crystallogr.* **A24**, 321-324.

Foit, F.F., Jr. (1989): Crystal chemistry of alkali-deficient schorl and tourmaline structural relationships. *Am. Mineral.* **74**, 422-431.

——— & Rosenberg, P.E. (1979): The structure of vanadium-bearing tourmaline and its implications regarding tourmaline solid-solutions. *Am. Mineral.* **64**, 788-798.

Fortier, S. & Donnay, G. (1975): Schorl refinement showing compositional dependence of the tourmaline structure. *Can. Mineral.* **13**, 173-177.

Grice, J.D. & Robinson, G.W. (1989): Feruvite, a new member of the tourmaline group, and its crystal structure. *Can. Mineral.* **27**, 199-203.

Hawthorne, F.C. & Grice, J.D. (1990): Crystal structures analysis as a chemical analytical method: application to light elements. *Can. Mineral.* **28**, 693-702.

———, MacDonald, D.J. & Burns, P.C. (1993): Al/Mg disorder in the crystal structure of dravite. *Am. Mineral.* **78**, 265-270.

Nuber, B. & Schmetzer, K. (1981): Strukturverfeinerung von Liddicoatit. *Neues Jahrb. Mineral., Monatsh.*, 215-219.

——— & ——— (1984): Structural refinement of tsilaisite (manganese tourmaline). *Neues Jahrb. Mineral., Monatsh.*, 301-304.

Pouchou, J.L. & Pichoir, F. (1984): A new model for quantitative analysis. I. Application to the analysis of homogeneous samples. *La Recherche Aerosp.* **3**, 13-38.

——— & ——— (1985): "PAP" $\phi(\rho Z)$ procedure for improved quantitative microanalysis. *Microbeam Anal.*, 104-106.

Rossman, G.R. & Mattson, S.M. (1986): Yellow, Mn-rich elbaite with Mn–Ti intervalence charge transfer. *Am. Mineral.* **71**, 599-602.

Schmetzer, K. & Bank, H. (1984): Crystal chemistry of tsilaisite (manganese tourmaline) from Zambia. *Neues Jahrb. Mineral., Monatsh.*, 61-69.

———, Nuber, B. & Abraham, K. (1979): Zur Kristallchemie Magnesium-reicher Tourmaline. *Neues Jahrb. Mineral., Abh.* **136**, 93-112.

Shigley, J.E., Kane, R.E. & Manson, D.V. (1986): A notable Mn-rich gem elbaite tourmaline and its relationship to "tsilaisite". *Am. Mineral.* **71**, 1214-1216.

Received August 24, 1992, revised manuscript accepted March 17, 1993.